Exploring the 65nm frontier of alternating phase shifting masks with a quartz dry etch chemistry

S. A. Anderson, Applied Materials, Inc.; R. Neubauer, Advanced Mask Technology Ctr. GmbH & Co. KG (Germany); A. Kumar, I. Ibrahim, Applied Materials, Inc.

ABSTRACT

Advances in photo mask etch technology are clearing the way for 65nm alternating phase shifting masks (alt-PSM) to be used as a principal component in a typical mask set. As wafer features shrink to ever smaller sizes, the specifications on the photo mask etch performance become more and more stringent. To meet the challenging demands of 65nm technology, alt-PSM's are employed to help deliver a reliable and repeatable pattern transfer to the wafer. Hence, especially in the framework of quartz dry etch technology for the production of high-end alt-PSM's ever tightening specifications generate various efforts of machine vendors and mask making industry to meet the demands [1].

This paper covers data from a ten experiment two level three factorial Design of Experiment. Therein, the effects of changing quartz process conditions (i.e., ICP power, RIE power, and gas chemistry) on the Applied Materials Tetra™ II Photomask Etch System were investigated. As for alt-PSM's the universally agreed upon number one priority is phase angle uniformity followed closely by RIE lag, sidewall angle (SWA), and micro-trenching this was also taken into account during the optimization process of the DoE findings.

The results show phase angle uniformity of less than 2.0° relative to a 180° etch depth and acceptable performance for RIE lag, SWA, and micro-trenching.

Trends and graphs of the DoE are presented and discussed in detail.

Keywords: alt-PSM, dry etch, etch rate uniformity, mask etch, micro-trenching, phase angle uniformity, phase shift, quartz etch, RIE Lag

1. INTRODUCTION

The criteria for developing phase shifting masks are some of the most stringent in the semiconductor etch arena. As a result, the practice of improving the pattern transfer to the wafer through the use of alternating phase shift masks (alt-PSM) is gaining more and more attention. When feature sizes on the wafer approach the wavelength of light being used in the lithography step, such as the 193nm wavelength for ArF lithography, the potential for the pattern to distort, shorten, or blur increases dramatically. By using alt-PSMs, or quartz phase shifting masks, 180° phase shifted transmission of the lithography laser is created at alternating features on the mask utilizing interference effects to enhance the contrast at the wafer.

This work is based on previous experiments on the Tetra™ II Photomask Etch System [1]. Hardware optimizations have improved the overall phase uniformity by minimizing the radial component of the etch rate from previous studies. Process exploration and optimization described here was carried out on the latest hardware configuration.

2. METHODOLGY

2.1 Mask patterning and preparation

Photomask blanks were sputtered with 70 nm CrO_xN_y/Cr (Hoya) and then coated with 300 nm of Fujifilm FEP-171 chemically amplified resist for the DoE and optimization. Pattern generation was completed using an Applied Materials ALTA 4300 creating a test pattern with an 11 x 11 layout, a 6 x 6 clear area in the upper left quadrant of the mask and a quality area of 132 x 132 mm^2. Global chrome load for the masks was 13%. For a more detailed description of the standard mask test vehicle and the experimental methods see the previous work [1].

2.2 Experimental design

Previous quartz etch development has shown that very good phase angle uniformity can be achieved at the low pressures achievable by the Tetra™ Photomask Etch System. Phase angle uniformity typically is the highest priority performance criteria for alt-APSM. For this two-level, three-factor full factorial design of experiment (DoE), gas ratio ($C_xH_yF_z$ to C_xF_y, where x, y, and z are specific to each molecule), bias power, and source power were varied. Pressure, gas flow, and source coil ratio have been fixed throughout the experiment. Performance criteria investigated were phase uniformity/range, reactive ion etch lag (RIE Lag), sidewall profile, micro-trenching and etch rate.

The design was chosen to allow the modeling of the most important factors impacting uniformity, RIE Lag, micro-trenching, sidewall profile and etch rate. The JMP™ v.5.0 Professional Edition from SAS Institute [2] was used in the analysis of the experimental data. Main factor trend data is presented in a manner that shows model predicted trends at the matrix center-point for process parameters. Table 1 lists control parameter variables, constant process parameters and measured response variables.

Table 1: Variables and corresponding levels tested, and the measured responses.

Process Control Parameter Variables	
	Units
Source Power	Watts
Bias Power	Watts
Gas Ratio	unitless
Constant Process Parameters	
	Units
Pressure	mTorr
Total Gas Flow	sccm
Source Coil Ratio	unitless
Measured Response Variables	
	Units
Uniformity/Range	deg.
RIE Lag	deg.
Sidewall Profile	deg.
Micro-trenching	% Etch Depth
Etch Rate	Å/s

2.3 Equipment

The etch experiments were performed in the Applied Materials Systems Tetra™ II Photomask Etch System powered by an inductively coupled plasma (ICP) source. The RF source is driven with a single RF generator, which allows for source current splitting between a smaller diameter inner coil and a larger diameter outer coil. The RF current splitting allows for flexible control of the power distribution to the coils and adds an increased level of control for plasma uniformity within the chamber. An independently controlled bias generator, phase-locked with the source generator, is used to control ion kinetic energy to the mask. The chamber was evacuated using a 2500 l/s turbomolecular pump backed by a dry mechanical pump. Process gases were injected into the chamber using an advanced gas injector system incorporated into the chamber lid.

2.4 Metrology

Resist etch depth and selectivity measurements were made for the FEP resist using the n&k Analyzer 1512 RT. Thickness measurements were taken at 121 locations covering a 132mm x 132mm area. Resist and chrome were dry-stripped after etch using a standard O_2 strip discharge for resist and Cl_2/O_2 strip discharge for chrome developed to minimize the strip effect on the quartz etch. Following the resist and chrome strip, the masks were wet cleaned using a sulfuric acid bath to remove all remaining residue on the quartz surface. Phase angle measurements for global uniformity were made using the Lasertec MPM-193 phase shift measurement system. RIE lag measurements were made using the FEI Stylus NanoProfilometer (SNP 9000) equipped with a 120nm x 120nm diamond tip. Cross section SEM images were collected using the Hitachi - SEM 4500.

3. RESULTS

A summary of the results are present here for the performance parameters of phase angle range, quartz etch rate, RIE lag, micro-trenching and sidewall angle. For each response, a model was generated using the JMP software [2]. The objective was to generate a model the best fit and minimum number factors and interactions contributing to the model. Prior to analysis, all results were normalized to 180° etch depth. The correlation coefficient, R^2, was greater than 0.94 for all models generated. In all main factor trend plots presented in this work, the DoE center-point is the reference process recipe.

3.1 Phase Angle Uniformity/Range

Nearly always considered the most important etch performance criterion in production, phase angle range is the measure of how the quartz etch rate for a given feature size changes over the global area of the mask; in this case, 132x132mm^2. By changing the process parameters in this experiment, it was possible to tune the phase angle uniformity to conditions where (1) the etch rate was faster in the center of the mask and (2) the etch rate was faster at the edge of the mask. For purposes of the model, the measured phase angle range for a center fast uniformity map was labeled as negative phase range; phase range for a center slow uniformity map was labeled as positive. All ranges were normalized to 180° etch depth.

The primary factors influencing phase uniformity are the source power and the bias power. Source power is the strongest main factor effect and created a more center slow etch pattern with increasing source power. Figure 1 shows the main factor trend plots generated from the model with the DoE center-point recipe as the reference. Bias power has the opposite effect generating a more center fast uniformity pattern at higher bias powers. It is known that SiO_2 etching in fluorocarbon discharges depends on both ion assisted etching and polymer film deposition. For certain conditions, the process is strongly dependent on the ratio of Fluorine to Carbon (F/C) which determines whether etching or deposition is the dominant process [3, 4]. Ions are generated from the collisions between plasma electrons and neutral gas particles within the chamber. At higher bias powers and a more anisotropic ion transport, the etch rate uniformity will more strongly reflect the ion distribution of the plasma—center fast for this process regime. The radicals that lead to polymerization on the mask are generated from collisions between incident electrons and neutrals. The result is a

dissociation of the gas into CF_x radicals and other polymerizing species where etch products from the resist also contribute to the polymerization.

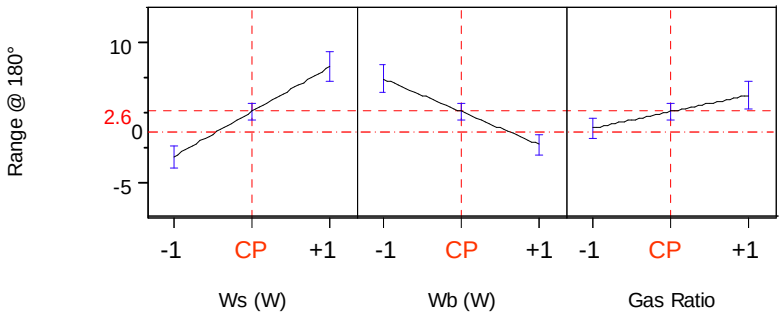

Figure 1: Main Factor Trend Plots for Phase Angle Range.

At low bias powers the kinetic energy of the reactive ions is reduced, and the ion trajectories are more isotropic. At higher source powers the rate of polymerization is increased due to the higher electron density which generates more radicals. Experimental results show that a center fast etch uniformity can be achieved by increasing the ion kinetic energy and ion flux to the mask. In contrast, a center slow etch signature can be achieved by increasing the number of radicals impinging on the surface through increased source power. Summarizing, a balance between ion and radical transport must achieved by tuning both source and bias power in order to minimize phase angle range over the mask. Figure 2 below compares two contour plots of phase angle data for run (a) with high source power and low bias showing a center slow etch rate and run (b) with low source and high bias power resulting in a center fast etch pattern. Etching to 180° from all the experimental runs, the best phase angle range obtained was 1.9° (1.0%) over 132x132mm^2 and a 3σ uniformity value of 1.5° (0.8%).

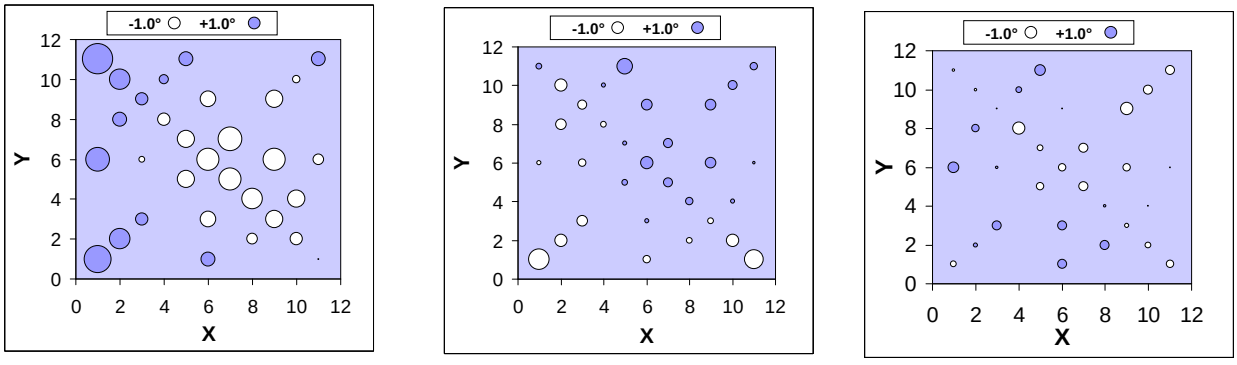

(a) **(b)** **(c)**

Figure 2: Phase uniformity plots showing (a) center-slow etch footprint, (b) center-fast etch footprint and (c) best overall phase range (1.9°).

Generally, the influence of the gas ratio has a minor effect in our study. Only in the case of low bias power and high gas ratio (low F/C ratio) is a significant effect visible. This results in an undesirably high phase angle range and a center-slow footprint, as shown in Figure 2 (c). We attribute this significant influence on phase angle range to the dominating deposition behavior of the plasma under these conditions.

3.2 Quartz Etch Rate

As one might expect, the same factors that have a strong influence on the global phase angle uniformity, also known as etch rate uniformity, have a strong influence on the etch rate itself. Hence, the significant parameters for etch rate turn out to be source power, bias power and the interaction between these two main factors. Gas ratio did not factor into the model for quartz etch rate.

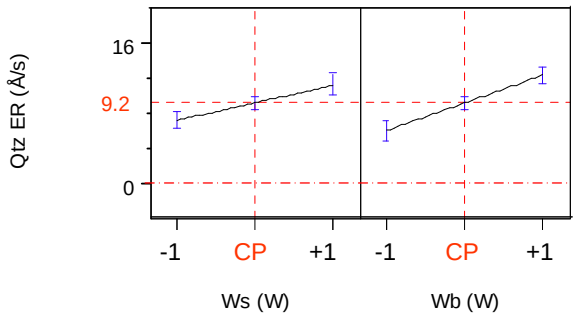

Figure 3: Main Factor Trend Plots for Quartz Etch Rate.

At lower bias powers both the anisotropic ion flux to the mask and ion kinetic energy are reduced. Radical flux to the mask due to isotropic transport is relatively unchanged and the etch rate decreases as a result of the interplay between polymerizing radicals and the smaller number and energy of etching ions. As source power is increased the ion density and number of radicals increase in the discharge. The increased ion flux to the mask increases the etch rate. At lower bias powers, under the proper conditions, where the ion kinetic energy is low enough and the polymer deposition dominates, the process can be flipped from etching to deposition. The result is expected, as reducing ion kinetic energies under the proper gas phase conditions have been shown to halt the etch process [5]. At low kinetic energy only a small amount of ions have enough kinetic energy to induce the etch of the mask. The polymer deposition during the time between incident etchant ions is such that the polymer buildup reaches a point where the etching is completely inhibited by the polymer [6]. In this experiment we approach this limit at low bias (low ion flux) and high source power (high number of radicals) where the observed etch rate was < 2.0Å/s.

3.3 RIE Lag

Reactive Ion Etch Lag or phase angle linearity is the quantitative measurement of the vertical etch rate for small CD features relative to the vertical etch rate for large CD features. In this work, the vertical etch depth was measured using the SNP 9000 for feature CD sizes between 300 nm and 2.5 microns. The RIE lag was normalized for 180° etch depth.

In comparing RIE lag high load and low load performance, the most striking result is the independence of the process trends on the asymmetric loading of the mask. Trends for source power, bias power and gas ratio were similar in both the high load and low load regions. This is confirmed from further studies (not shown) that loading plays a minor role in the RIE lag data which is important when transferring the etch process from a test pattern to a production mask. This makes life easier during production when one recipe can be employed for all loadings. Main factor process trends are presented in Figure 4.

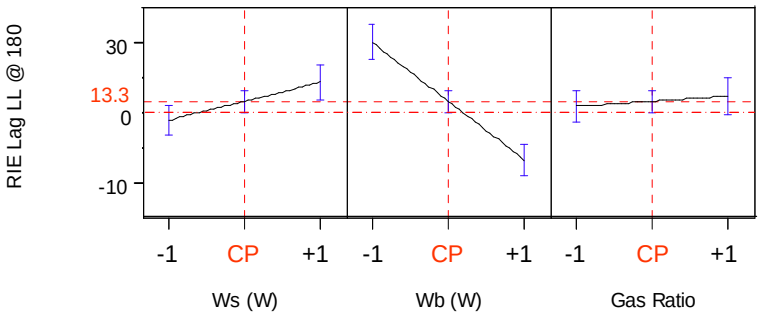

Figure 4: Main Factor Trend Plots for RIE Lag.

The most important effect is the bias power, where the gas ratio plays only a minor role. Increasing the bias power, independent of source power and gas ratio, decreases the RIE lag. At very high bias power, we even see a flip of the RIE curvature from a conventional to an inverse RIE lag where the smaller features etch faster than the larger features. From post DoE confirmation experiments the flip of the RIE lag curve for a bias power change from medium to high bias, is observed to change from a positive slope to negative slope, as expected.

With increasing bias power ion trajectories to the trench become more anisotropic as ions are accelerated through the sheath. The ion transport becomes less dependent on the feature size as ion kinetic energy increases and more ions reach the trench bottom. On the other hand, deposition is mainly contributed by radicals and are unaffected by the increase in the bias power induced E-field [7]. Therefore, the radicals move isotropically and small feature sizes show a smaller effective open angle for constant trench depth. The effect of the radicals decreases with shrinking feature size. This means that at small feature size and high bias power, the etching effect of the high kinetic energy ions dominates the overall process behavior [8].

At low bias power, the ion trajectories are more isotropic and have lower kinetic energies than at higher bias powers. Due to the higher aspect ratio of the small features combined with the less anisotropic ion trajectories, the transport of ions to the trench bottom is less efficient resulting in a reduced etch rate in comparison to the larger features. These larger features are less affected by the decreased anisotropy of the ions. Summarizing, the small features etch more slowly than the large features at low bias power resulting in positive or conventional RIE lag [7].

Finally, at low bias powers, the RIE is very positive. $C_xH_yF_z$ chemistries are known to be able to flip from etching to deposition mode at very low bias powers, where the ion kinetic energy drops below an etch threshold energy. Especially at very low bias power, not only are the ions less anisotropic, but the ion kinetic energy is so low that the ion energy drops below an etch threshold energy and the plasma species no longer contribute to etching [5]. At very low bias powers, the plasma species deposit polymer on the mask.

3.4 Micro-trenching

Small features forming trench-like structures in the corner of the trench where the sidewall meets the trench bottom are commonly referred to as micro-trenching. These micro-features have a negative effect on the pattern transfer of the mask and therefore it is desirable to produce masks where micro-trenching is minimized or eliminated all together. Various mechanisms have been proposed as the cause of micro-trenching including surface diffusion of etchants [9, 10], shadowing of neutral deposition precursors [11], deflection of ions from sidewalls [12] and differential charging of the etch features [13]. Schaepkens et al.[13] showed that micro-trenching varies greatly with bias frequency, suggesting that the effect is primarily an ion effect. They postulate that micro-trenching is largely influenced by the differential scattering of ions to the trench bottom. The scattering results from a positive charge buildup at the trench floor from etchant ions and a

negative charge buildup on the sidewalls from incident electrons, thus defining the potential differential causing micro-trenching [13].

In this work, micro-trenching is quantitatively evaluated by measuring the depth of the micro-trench relative to the average trench depth. In this analysis, the depth was measured as a negative depth for comparison purposes. The three main factors and the interaction between source and bias power are significant for micro-trenching. Cross section images of the two experiments are shown in Figure 5.

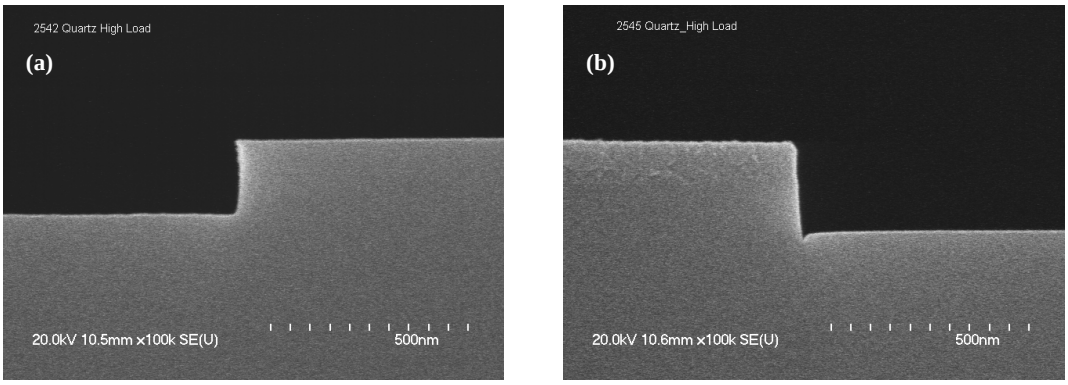

Figure 5: Cross-section SEM Data showing (a) no micro-trenching (Cr stripped) and (b) large micro-trenching (Cr in image).

From the model, the most striking results are when comparing the micro-trenching trend data to the RIE response curves. From the comparison of the RIE lag and micro-trenching trend data, there is a clear correlation between RIE lag response and micro-trenching response curves. For each and every factor in this study, the response is such that increasing conventional RIE lag results in more shallow micro-trenching. This is strong evidence that further supports that ion energy and the polymer deposition have effects on both micro-trenching and RIE Lag showing that the underlying mechanisms are strongly correlated for the two. Trend plots for micro-trenching are show in Figure 6.

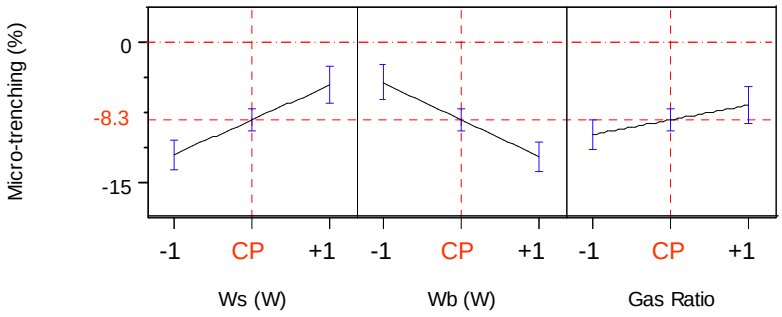

Figure 6: Main Factor Trend Plots for Micro-trenching

Higher bias power increases the kinetic energy of the ions resulting in an increased etch rate for small features relative to the large features (i.e., less positive or more inverse RIE lag). At the same time, higher bias power increases the number of the ions impinging on the surface. The increased ion flux to the mask results in more ions deflected towards the corners producing micro-trenching and more ions available for creating the positive trench potential. On the other hand, with a higher ion kinetic energy the magnitude of the micro-trenching is increased. Given the assumption that the

polymerization is driven by radicals (independent of bias power) [7], we can explain the increased micro-trenching at higher bias power purely to a higher impact energy of the ions to the surface.

3.5 Sidewall Angle

The variability in the shape of the sidewall and the subjective measurement method in determining the side wall angle results in some diversity of the measured side wall angle value for a given mask. However, based on the results from the cross section SEMs for the DoE runs, we see that bias power is the major contributor. Interestingly, with increasing anisotropy we see a decreasing side wall angle with increasing bias power. This suggests that the anisotropy of the ions is not the dominant factor affecting the sidewall angle. Finally, source power and gas ratio can have a substantial effect on the side wall angle, as well.

3.6 Process optimization

Typical performance specifications for alt-PSM applications call for phase uniformity ranges of < 2.0°. From the investigations in this work we see that in order to achieve the process performance necessary to meet 65nm process performance, a balance must be struck between the polymerizing and RIE characteristics of the discharge. The DoE model provides a powerful tool for predicting and optimizing the quartz etch process. By including uniformity range, RIE lag, micro-trenching, sidewall angle and etch rate into the prediction engine of the DoE software, two optimization runs were generated. The first of these runs, recipe A, was processed at medium source power, high bias power, and high gas ratio. Results for run A are shown in Figure 7.

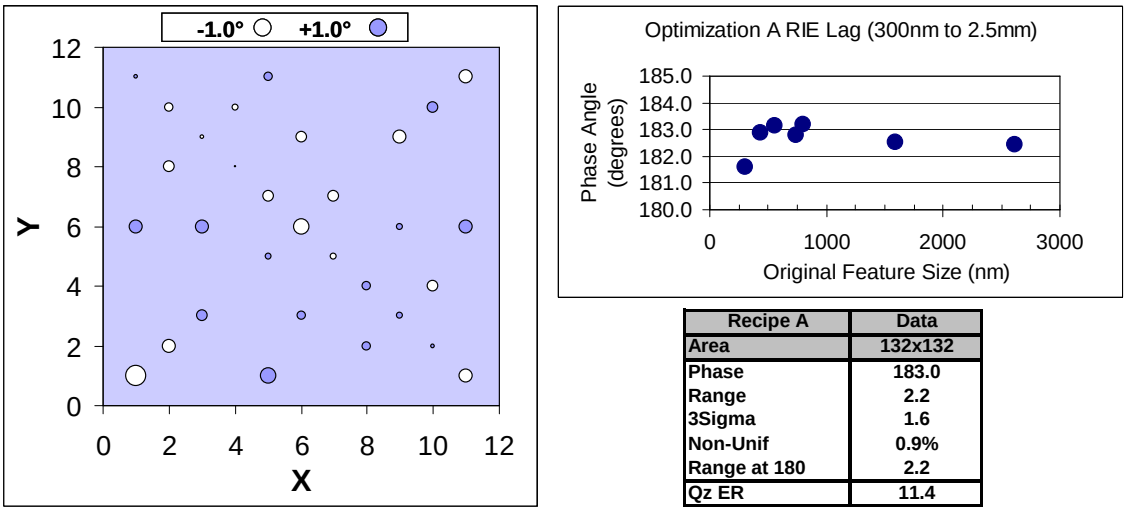

Recipe A	Data
Area	132x132
Phase	183.0
Range	2.2
3Sigma	1.6
Non-Unif	0.9%
Range at 180	2.2
Qz ER	11.4

Figure 7: Optimization Run A (Med Source Power, High Bias Power, and High Gas Concentration) resulting in 2.2° phase angle range (31 data points, 132x132mm^2) and 2.0° RIE Lag.

The overall phase angle performance for run A was excellent with a phase angle range of 2.2° and a RIE lag of 2.0° from 300nm to 2.5μm. Sidewall profiles for run A was ~87° with a negligible amount of micro-trenching.

Balancing the polymer deposition with etching was shown to be related to the amount of radical formation in the discharge and the ion kinetic energy and flux to the mask. For the second optimization run, bias power was increased to improve the overall phase angle uniformity (see Figure 1) and to optimize RIE lag (see Figure 4). In order to maintain

the acceptable level of micro-trenching in run A, source power was increased. Optimization run B was run at high source power, higher bias power, and a lower gas ratio in comparison to optimization run A. Results for run B are shown in Figure 8.

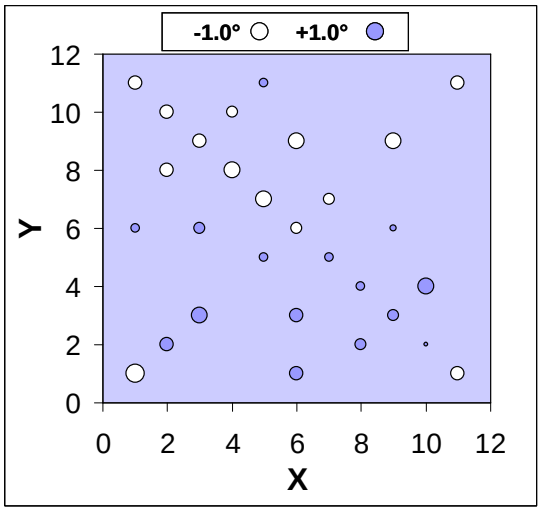

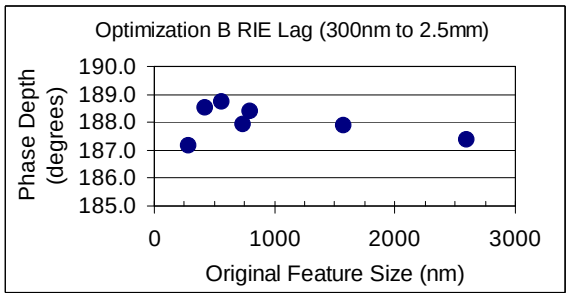

Recipe B	Data
Area	132x132
Phase	187.7
Range	2.0
3Sigma	1.7
Non-Unif	0.9%
Range at 180	1.9
Qz ER	14.3

Figure 8: Optimization Run B (High Source Power, High Bias Power, and Low Gas Concentration) resulting in 1.9° phase angle range (31 data points, 132x132mm^2) and <2.0° RIE Lag (300nm to 2.5μm).

Optimization for run B resulted in a phase angle range of 1.9° and a RIE lag range of < 2.0°, both meeting 65nm node specifications. Sidewall angle for run B is 89° with a marginal increase in micro-trenching. The etch rate for run B is increased to > 14Å/s which makes targeting 180° etch depth more challenging, but the stability of the Tetra™ II Photomask Etch System improves the ability to etch to the target depth.

4. CONCLUSIONS

Ultimately, the goal of process development is to explore the process window and gain a better understanding of the process so that etch performance is improved. Phase shifting masks require extreme levels of performance control as evidenced by the 2.0° phase uniformity criterion. For the quartz etch process described here, we identify main process factors affecting phase uniformity, RIE lag, etch rate, micro-trenching and sidewall profile. Bias power and source power dominate the effects in this study. Gas ratio does not appear in the phase uniformity model and plays only a minor role in the remaining process performance criteria. Micro-trenching and RIE lag are affected by the same process mechanisms.

Understanding the process trends is only part of the equation. From the analysis here we are able to model each of the desired response variables and use these models to predict future process performance during the optimization stage as well as to control the process. This allows us to switch the uniformity profile from center slow to center fast (see Figure 2) as well as to change RIE slope from conventional to inverse curvature.

The trends derived from the DoE model facilitated process optimizations resulting in two recipes, A and B. Both successfully met typical specifications for next generation photomask applications. Based on these runs, the Tetra™ II Photomask Etch System is capable of providing less than 2° phase angle uniformity and 2° RIE lag with good sidewall profiles and reasonably limited levels of micro-trenching providing the best quartz dry etch solution for 65nm alt-PSM applications.

5. ACKNOWLEDGMENTS

The authors would like to thank E. Gabriel, R. Wong, and R. Vinulan for their assistance in completing these experiments, C. Collard and M. Chandrachood for their useful insight and discussions and Josef Mathuni and Guenther Ruhl for their technical expertise and assistance.

6. REFERENCES

1. S. A. Anderson, et. al., SPIE Proc., **66**, 5256 (2003).
2. SAS Institute, SAS Campus Drive, Cary, NC.
3. H. Shan, B. K. Srinivasan, D. W. Jillie, Jr., J. S. Multani, and W. J. Lo, J. Electrochem. Soc., **141**, 2904 (1994).
4. J. W. Coburn and E. Kay, IBM J. Res. Dev., **23**, 33 (1979).
5. G. S. Oehrlein, Y. Zhang, D. Vender and O. Joubert, J. Vac. Sci. Technol. A **12**, 333 (1994).
6. M. Matsui, T. Tatsumi and M. Sekine, Plasma Sources Sci. Technol., 11, A202 (2002).
7. R. A. Gottscho, C. W. Jurgensen, and D. J. Vitkavage, J. Vac. Sci. Technol. B, **5**, 2133 (1992).
8. M. J. Buie, A. M . Joshi and J. Regis, Electrochem. Soc., **96**, 469 (1996).
9. M. Sato and Y. Arita, J. Electrochem. Soc. **134**, 2856 (1987).
10. N. I. Maluf, S. Y. Chou, J. P. McVittie, S. W. J. Kuan, D. R. Allee, and R. F. W. Pease, J. Vac. Sci. Technol. B **7**, 1498 (1989).
11. M. F. Doemling, N. R. Rueger, and G. S. Oehrlein, Appl. Phys. Lett. **68**, 10 (1996).
12. A. C. Westerheim, A. H. Labun, J. H. Dubasch, J. C. Arnold, H. H. Sawin, V. Yu-Wang, J. Vac. Sci. Technol. A **13**, 853 (1995).
13. M. Schaepkens and G. S. Oehrlein, Appl. Phys. Lett, **72** 1293 (1998).